Proceedings of CECNet 2022
A.J. Tallón-Ballesteros (Ed.)

doi:10.3233/FAIA220576

Time-Domain Feature Parameter Extraction Algorithm of Pulse Wave Based on Morphological Features

Xingguang Geng[a,b], Yitao Zhang[a,b,1] ,Jun Zhang[a,b],Yunfeng Wang[a,b] and Haiying Zhang[a,b2]
[a] *Institute of Microelectronics of Chinese Academy of Sciences, China*
[b] *University of Chinese Academy of Sciences, China*

Abstract. Pulse wave's Time-domain characteristics have clear physiological and pathological significance, and are widely used in pulse recognition and disease prediction. At present, for different forms of pulse wave feature points, the accuracy of time-domain feature point extraction algorithms varies greatly. Therefore, this paper proposes a time-domain feature extraction algorithm of pulse wave based on morphological features. Firstly, the pulse wave is normalized and averaged by using normalization and correlation averaging methods. Secondly, the morphological characteristics of the main wave are divided into two states: extreme point and non-obvious feature. The characteristic morphology of the dicrotic front wave and the dicrotic wave are divided into three states: extreme point, non-obvious feature, feature fusion or disappearance. Finally, the location range of each feature point is determined, and the pulse wave feature points are identified by the curvature method and the difference method. The experiment shows that the algorithm can effectively identify the pulse wave characteristic points of common pulse waves, which creates conditions for the effective extraction of subsequent relevant human physiological and pathological information.

Keywords. pulse wave, time-domain characteristics, morphological characteristics, extreme point, dicrotic front wave, dicrotic wave

1. Introduction

Pulse wave carries important physiological and pathological information of human body[1-3]. At present, the methods of extracting pulse wave feature parameters mainly include time-domain, frequency-domain and time-frequency domain feature parameters. [4, 5] Because time-domain feature parameters are intuitive and each feature point has clear physiological significance. Therefore, they are widely used in pulse recognition and disease prediction [6, 7]. As shown in fig.1, the time-domain characteristics mainly

[1] Corresponding Author, Yitao Zhang (Institute of Microelectronics of the Chinese Academy of Sciences, Beijing 100029, China; University of Chinese Academy of Sciences, Beijing 100049, China) and E-mail: zhangyitao@ime.ac.cn.
[2] Corresponding Author, Haiying Zhang (Institute of Microelectronics of the Chinese Academy of Sciences, Beijing 100029, China; University of Chinese Academy of Sciences, Beijing 100049, China) and E-mail: zhanghaiying@ime.ac.cn.

include five feature points: the main wave peak (c), the dicrotic front wave valley (d), the dicrotic front wave peak (e), the dicrotic wave valley (f) and the dicrotic wave peak (g).[8]

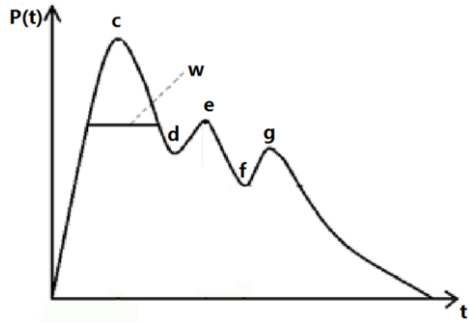

Figure1. Time-domain characteristic parameters of pulse wave

At present, the methods of extracting time-domain feature parameters mainly include slope method, slope and threshold combination method, differential method, extreme value method, wavelet method, sentence pattern method, etc. The slope method is mainly used to find the slope change point to determine the characteristic pulse wave. This method has poor recognition effect for waveforms with insignificant slope change or large pulse wave interference. The slope and threshold combination method is mainly based on the slope method to determine the location of feature points by determining the range of time-domain features[9].This algorithm can only identify the feature points of a certain type of pulse wave. When the pulse wave is relatively gentle, the recognition effect is not ideal[10]. The differentiation method is to use the spline function to obtain the differential diagram of a single cycle pulse wave, set the threshold, and take the position of the first zero crossing point after differentiation as point c, and the rest are points d, e, f and g in turn. This method is only applicable to the case that both the dicrotic front wave and the dicrotic wave have wave peaks and valley, but the value of the first zero crossing point is not necessarily point c. The extreme value method is to calculate the maximum value in the pulse wave, take the first maximum point as point c, and then find the second largest and third largest extreme points as point e and point g in reverse order. Like the differential method, this method ignores that the maximum point is not necessarily point c, and the method has a large error when some people's the dicrotic front wave and the dicrotic wave are not obvious. Wavelet transform mainly uses wavelet transform to highlight time-domain feature points (such as Gaussian wavelet) and extract time-domain feature points. However, this method has poor recognition effect on d and e points [11, 12]. The main idea of syntactic pattern recognition is to classify and process the pulse wave signals, and then extract the characteristic parameters of the classified pulse wave signals. Therefore, it is necessary to establish an accurate classification standard for single cycle pulse waves, which has certain difficulties in the actual situation [13, 14]

In this paper, we summarize the morphological characteristics of pulse wave, and propose a time-domain feature extraction algorithm based on the characteristic morphology. Firstly, the pulse wave is normalized and averaged by using normalization and correlation averaging methods. Secondly, the morphological characteristics of the main wave are divided into two states: extreme point and non-obvious feature. The characteristic morphology of the dicrotic front wave and the dicrotic wave is divided into

three states: extreme point, non-obvious feature, feature fusion or disappearance. Finally, the location range of each feature point is determined, and the pulse wave feature points are identified by curvature method and difference method. The accurate identification of pulse wave feature points is helpful to the early prevention, diagnosis and follow-up treatment of diseases, which is of great clinical significance.

2. Materials and Methods

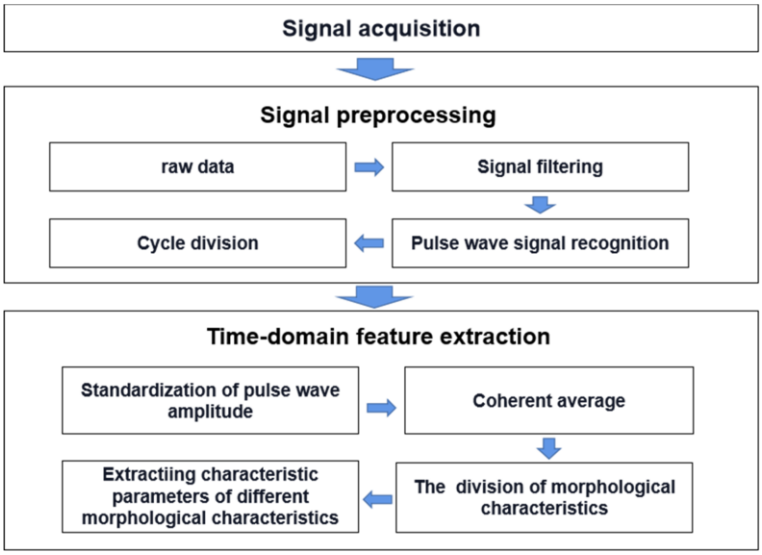

Figure2. Flow Chart of Pulse Wave Collection and Processing

This section mainly contains the following three parts. The first is signal acquisition, which mainly uses signal acquisition devices to collect pulse wave data. The second is signal preprocessing, which mainly uses filtering algorithms, pulse wave recognition algorithms, and cycle division algorithms to complete signal filtering, pulse wave signal recognition, and pulse wave cycle division. The last is time-domain parameter extraction, which is mainly used to standardize and average pulse waves, and classify pulse waves according to their morphological characteristics, Then the characteristic parameters of pulse wave are extracted by classification. Fig.2 shows the flow chart of pulse wave collection and processing.

2.1. Signal acquisition

As show in fig.3(a), in this paper, we use flexible bionic multi-channel pulse acquisition instrument to obtain pulse wave data. As show in fig.3-(b), the acquisition probe of the pulse diagnostic instrument contains compound pressure sensors, each of which is composed of a static sensor and a flexible dynamic sensor, and can complete the synchronous acquisition of static pressure and pulse wave. Through the way of air bag pressurization, simulating the pressurization technique of pulse taking in traditional Chinese medicine, the synchronous gradient pressurization and synchronous signal acquisition of the three positions can be realized. The sampling frequency is 225Hz. The

range of air bag pressurization is 10-150mmhg. And the pressurization gradient is 10mmHg. The static pressure signal and pulse wave signal in 10s are collected under each pressure. Fig.3-(c) shows single channel pulse sensor signal.

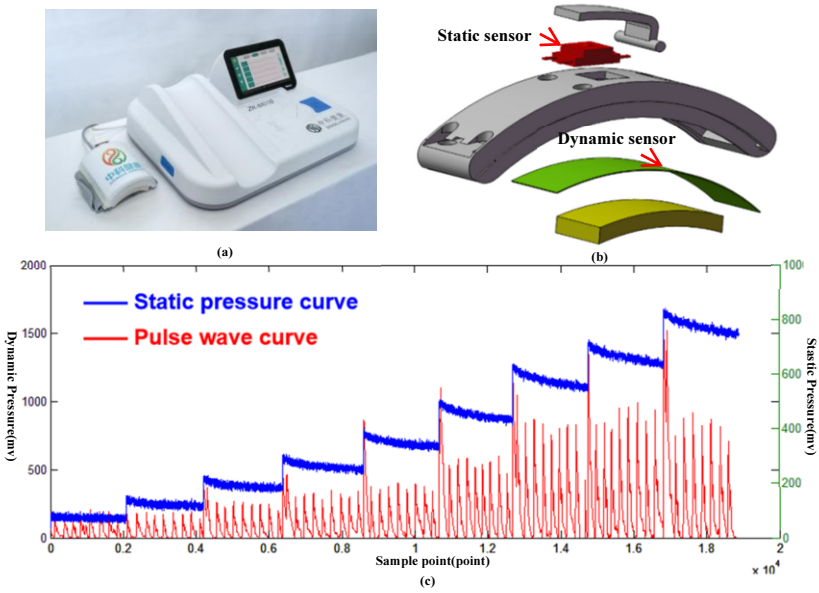

Figure 3. (a)Multi channel pulse wave acquisition device.(b)A compound pressure sensor Structural drawing(c) Single channel pulse sensor signal.

2.2. Signal preprocessing

The signal preprocessing algorithm is mainly composed of three parts: signal filtering, pulse wave signal recognition and period division. Firstly, 50Hz notch filter is used to remove power frequency noise, and wavelet transform is used to remove EMG noise and respiratory noise. The deep neural network algorithm is used to complete the pulse wave signal recognition [15]. And finally, the differential threshold method is used to complete the single cycle pulse wave.

2.3. Time-domain feature extraction method

(1) Standardization of pulse wave amplitude

As the pulse wave is an unstable signal, the amplitude of the pulse wave will be slightly different. In order to eliminate the influence of the amplitude, the pulse wave needs to be standardized. The pulse wave signal is described as a function$y(n)$. The formula for standardization is as follows:

$$z(n) = \frac{y(n) - y(1)}{\max[y(N)] - y(1)}, n = 1,2,3 \ldots N \quad (1)$$

In the formula, $z(n)$is the pulse sequence function obtained after standardization. N is the number of sampling points. Before and after standardization are shown in fig.4-(a) and fig.4-(b).

(2) Coherent average

Pulse wave is a quasi-periodic physiological signal. In general, the pulse wave carries noise of different frequency ranges, and the filter method cannot remove it well. The method of multiple signal superposition can be used to increase the signal gain. This paper sets $y_i(t)$ to represent a single cycle pulse wave signal with certain noise, then

$$y_i(t) = s(t) + n_i(t) \tag{2}$$

Where: $s(t)$ refers to the useful signal that occurs repeatedly. $n_i(t)$ represents random noise. As shown in fig.4-(c), in this paper, three spline interpolation method is used to unify the sampling points of pulse wave. According to the above formula, the single cycle pulse wave signal is superposed for many times, and the expression is as follows:

$$\bar{y}(t) = \frac{1}{N}\sum_{i=1}^{N} y_i(t) = \frac{1}{N}\sum_{i=1}^{N}[s(t) - n_i(t)] = s(t) + \frac{1}{N}\sum_{i=1}^{N}[n_i(t)] \tag{3}$$

Where:$\bar{y}(t)$ is the average signal. N is number of sampling points after triple bound spline interpolation

Assuming that the power is expressed as P and the variance of $n_i(t)$ is expressed as σ^2, then for $y_i(t)$, its signal to noise ratio (SNR) can be expressed as:

$$SNR = \frac{P}{\sigma^2} \tag{4}$$

The formula shows that the noise variance will be reduced by N times by using the superposition averaging processing, and the pulse wave signal ratio will be increased by $\sqrt{N}$ times after using the averaging processing. The waveform after coherent average is shown in fig.4-(d) (red curve).

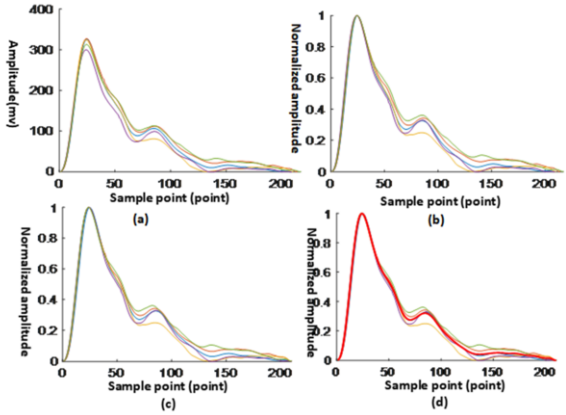

Figure 4. (a) Original pulse wave waveform (b) Amplitude standardized pulse wave waveform (c) Pulse wave waveform after resampling (d) Pulse wave waveform after coherent average

(3) The division of common pulse wave morphological characteristics

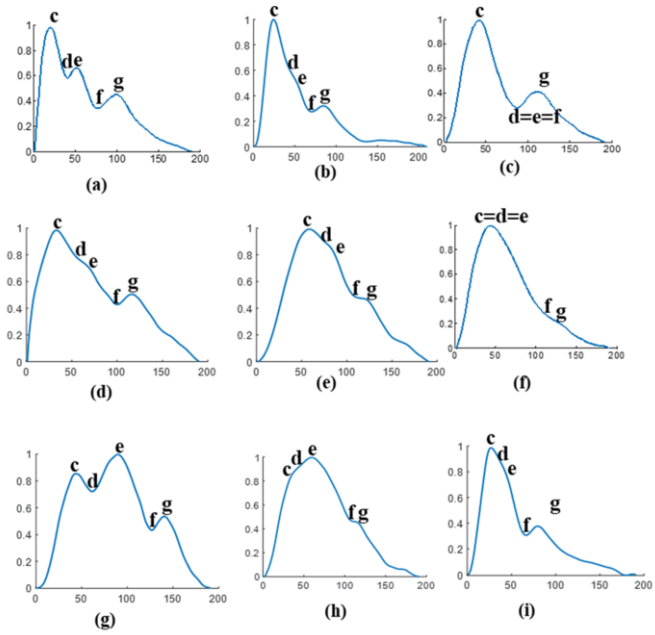

Figure 5. Common Pulse Wave Morphology

When the blood vessels have good elasticity and the human blood runs smoothly, generally speaking, the pulse wave of a complete cycle mainly includes three main characteristic waves: the main wave, the dicrotic front wave and the dicrotic wave, as shown in fig.5-(a). For some reason (such as high heat), the increase of blood flow in the cross-sectional area of the blood vessel within a unit time will enhance the local expansion and contraction ability of the human artery. The pulse wave shows that the dicrotic front wave is close to the dicrotic wave, as shown in fig.5-(b). When the blood vessel is further expanded, the dicrotic front wave will fuse with the dicrotic wave. At this time, the pulse wave presents double peaks, as shown in fig.5-(c). On the contrary, due to some reason (such as cold stimulation), the hardness of the human blood vessel wall increases. On the pulse wave, it is shown that the dicrotic front wave is close to the main wave peak, as shown in fig5-(d). When the hardness does not increase, the dicrotic front wave is fused with the main wave peak (as shown in fig.5-(e)), and even the position of the dicrotic front wave exceeds the main wave peak (as shown in fig.5-(f)).

It can be seen from fig.5 that the characteristic morphology of the main wave can be divided into two states: extreme point, non-obvious feature. And the characteristic morphology of the dicrotic front wave and the dicrotic wave can be divided into three states: extreme point, non-obvious feature, feature fusion or disappearance. Therefore, in the time domain feature recognition, it needs to be discussed according to the situation.

(4) Extraction of time-domain characteristic parameters of different morphological characteristics

Firstly, obtain the position of the heart splash point (b). As shown in fig. 6, for a single cycle pulse wave, there is a first-order difference maximum point between the maximum peak point of the pulse wave and the starting point of the pulse wave, and the maximum point is the heart splash point (point b). The main wave, the dicrotic front

wave and the dicrotic wave are all located on the right side. It is assumed that the data length of pulse wave y (n) is N. The expression of first-order differential d (n) is as follows:

$$d(n) = y(i+1) - y(i), \qquad i = 1,2 \ldots . N-1 \tag{5}$$

From the definition of each characteristic point, w is the width of the upper 1/3 of the main wave (expressed in g and k in the text). The effect is shown in fig. 6. The value of w_t is determined by the occurrence time of the dicrotic front wave and the peripheral resistance. Is calculated as follows,

$$w_t = \frac{y(k_x) - y(a_x)}{N}, \qquad i = 1,2 \ldots . N-1 \tag{6}$$

In the formula, k_x anda_x are the abscissa corresponding to point k and point a on the pulse wave respectively.

Point b is located between the starting point of the pulse wave and point a. According to that point b is the maximum value point of the first order difference of the pulse wave, we can obtain the abscissa of the pulse wave position point. Then the abscissa $b_x$of point b meets the following requirements:

$$\begin{cases} \mathrm{d}(b_x) - \mathrm{d}(b_x - 1) > 0 \\ \mathrm{d}(b_x) - \mathrm{d}(b_x + 1) > 0 \\ b_x > 0 \\ b_x < a_x \end{cases} \tag{7}$$

In the formula, b_x is the abscissa corresponding to point b on the pulse wave .

Secondly, calculate the maximum peak value point c', which is not necessarily the location of the main peak point. According to the definition, c' can be meet the following conditions:

$$\begin{cases} {c'}_x - {c'}_{x-1} > 0 \\ {c'}_x - {c'}_{x+1} > 0 \\ {c'}_x > b_x \\ {c'}_x < N \\ {c'}_y > y(n), n \neq {c'}_x \end{cases} \tag{8}$$

In the formula,${c'}_x$ is the abscissa corresponding to point c' .

Thirdly, obtain the position of f (the dicrotic wave valley) and g (the dicrotic wave peak) in the pulse wave.

Case1: If f and g are extreme points: when actually looking for f and g points, there are often multiple wave extreme points within the judgment range. In order to eliminate the influence of interference points, the maximum value of the difference between g and f's ordinates is often selected. At the same time, the abscissa positions of g and f points should be greater than the abscissa positions of c points, and the abscissa position of f point should be less than the abscissa position of g point. From this, the judgment formula of g point and f point can be obtained as follows:

$$\begin{cases} \mathrm{x}(g_x) - \mathrm{x}(g_x - 1) > 0 \\ \mathrm{x}(g_x) - \mathrm{x}(g_x + 1) > 0 \\ g_x > k_x \\ g_x < N \\ (g_y - f_{y)} \geq (p_y - v_{y)} \end{cases} \tag{9}$$

In the formula g_x is the abscissa corresponding to point g . f_y is the ordinate corresponding to point f.v represents a valley under certain conditions.$v_y$is the ordinate corresponding to point v.

Point f is located at the first valley point on the left side of the point g.

Case 2: If the f and g characteristics are not obvious.

Obtain the curvature transformation expression of $x(n)$ according to the curvature definition.

$$k(n) = \left(\frac{y_2}{1 + {y_1}^2}\right)^{1.5}, n = 1,2 \ldots . N \tag{10}$$

In the formula, y_1 is the first derivative of y.$y_2$is the second derivative of y. In order to remove the interference term in the curvature, the original curvature is smoothed by five points, which are determined by the sampling frequency of the original data. The filtering effect is shown in fig.6. In this paper, $fs = 225$. According to the characteristics of points g and f, if g and f are extreme points of curvature, then the positions of g and f will not exceed the maximum point c'. At the same time, points f and g are located on the right side of point k. The corresponding point f should be the maximum point of curvature. To sum up, we can get the curvature judgment method of point f:

$$\begin{cases} \mathrm{k}(f_x) - \mathrm{k}(f_x - 1) > 0 \\ \mathrm{k}(f_x) - \mathrm{k}(f_x + 1) > 0 \\ f_x > k_x \\ f_x < N \\ f_y \geq k(i), i = k_x, k_x + 1, \ldots . N \end{cases} \tag{11}$$

The minimum point of curvature wave crest on the right side of point f is point g. If there are no points g and f in the curvature, consider the third case, the dichroic wave and the dichroic front wave are merged.

Case3: the dichroic wave and the dichroic front wave are fusion or disappearance. According to the previous description, when the degree of vascular sclerosis increases, the dichroic wave will move to the dichroic front wave and even fuse. At this time, the position of the differential wave is merged with that of the heavy wave front wave.

$$\begin{cases} g_x = e_x \\ g_y = e_y \\ f_x = d_x \\ f_y = d_y \end{cases} \tag{12}$$

In the formula$e_x$and d_x is the abscissa corresponding to point$e$ and d.$e_y$is the ordinate corresponding to point e.

Lastly, obtain the positions of c (main wave peak), d （the dicrotic front wave valley） and g （the dicrotic wave peak） in the pulse wave.

Case1: the dichroic wave exists: if the dichroic wave exists, the location of the dichroic front wave should be in front of the dichroic wave valley, which is mathematically expressed as the abscissa position of the dichroic front wave is less than the abscissa position of the dichroic wave valley. Since the differential front wave is an extreme point or the feature is not obvious

When the differential front wave takes wave crest and wave valley as extreme points

$$\begin{cases} c = c' \\ y(e_x) - y(e_x - 1) > 0 \\ y(e_x + 1) - y(e_x) < 0 \\ e_x > k_x \\ e_x < f_x \end{cases} \tag{13}$$

At the same time, it is considered that there may be multiple peak points between the dichroic front wave and the main wave peak c in the pulse wave. According to the relevant regulations of the pulse wave, the first peak is the main wave peak, the last peak is the dichroic front wave peak, and the nearest wave valley point in front of the dichroic front wave peak is the wave valley point d of the dichroic front wave.

When the differential front wave features are not obvious. If there is a peak curvature point between a and f, there is also a peak curvature point between a and f. Then determine the size of the curvature peak point on both sides: if the curvature peak point between a and is smaller than the curvature peak point between a and f, or there is only a curvature peak point between a and f, then the judgment method for point c and point d is as follows:

$$\begin{cases} c = c' \\ k(d_x) - k(d_x - 1) > 0 \\ k(d_x + 1) - k(d_x) < 0 \\ d_x > k_x \\ d_x < f_x \end{cases} \tag{14}$$

Where point d is the maximum curvature point between point c' and point f, and point e is the minimum curvature point between point d and point$f$.

If the peak curvature point between a and c' is less than the peak curvature point between c' and f, or if there is only a peak curvature point between a and c', if the minimum value of the peak curvature point is p, then

$$\begin{cases} c = p \\ k(d_x) - k(d_x - 1) > 0 \\ k(d_x + 1) - k(d_x) < 0 \\ d_x > p_x \\ d_x < c'_x \\ e = c' \end{cases} \tag{15}$$

Case2: The dichroic wave merges with the main wave peak. When the degree of arteriosclerosis is high, the dichroic wave and the main wave peak fuse. At this time, the crest and valley points of the digital wave disappear and merge in c. The expression is as follows:

$$c = d = e = c' \tag{16}$$

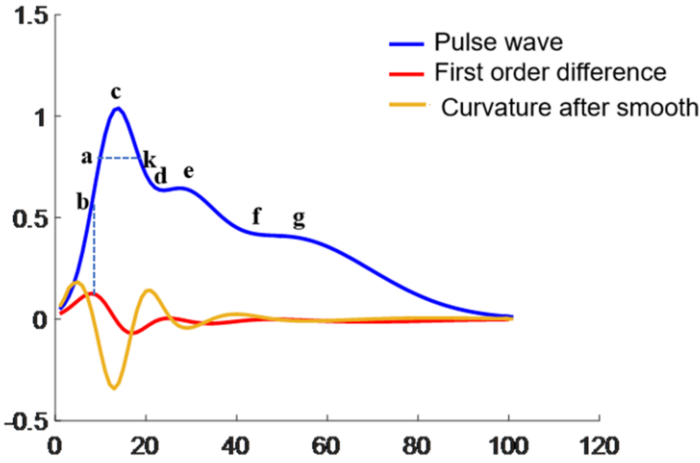

Figure 6. First order difference and smooth curvature of pulse wave

3. Experimental results

The students in our laboratory volunteered to participate in the experiment. Their age range is between 24 and 30 years old. In order to verify the accuracy of the time-domain feature extraction algorithm, we selected 9 groups of pulse waves as shown in fig.5. Use the manual calibration method to calibrate the pulse wave characteristics, and then use the algorithm in this paper to calculate. The comparison between the two is shown in table1. The number of data points is 190, and the sampling frequency is 225.

Table 1 Comparison between algorithm extraction and manual extraction (point=190, fs=225)

N	Algorithm identification results					Manual calibration results				
	T_{oc}	T_{od}	T_{oe}	T_{of}	T_{og}	T_{oc}	T_{od}	T_{oe}	T_{of}	T_{og}
a	20	41	52	77	101	20	41	52	77	101
b	26	45	51	71	87	26	42	51	71	87
c	28	71	71	71	96	28	71	71	71	96
d	33	53	66	99	117	33	52	66	99	117
e	59	73	81	113	119	59	72	82	112	119
f	44	44	44	114	129	44	44	44	114	128
g	45	62	89	126	141	45	62	89	126	141
h	35	47	59	109	114	33	49	59	108	111
i	27	37	44	66	80	27	34	42	66	80

It can be seen from fig.5 that (a) and (g) are the main wave peaks of the main wave, the dicrotic front wave and dicrotic wave. There is no difference in algorithm extraction

and manual extraction. It can also be seen from (g) that the main wave peak is not necessarily the highest point of the pulse wave peak in a cycle. In (b), (d), (e), (h) and (i), the characteristics of the dichroic front wave are not obvious, and there is no peak point. Then the accuracy of the identification algorithm extraction and manual extraction of point d and e is slightly different, with a maximum difference of two sampling points. The result is acceptable. In (f) and (h) the dichroic wave features are not obvious and there is no peak point, so the accuracy of the recognition algorithm extraction and manual extraction of f and g points is slightly different, with a maximum difference of two sampling points, and the results are acceptable. In general, the accuracy of the algorithm meets the requirements of data analysis.

4. Conclusion

In this paper, aiming at the time-domain characteristics of common pulse waves, combining curvature method and difference method, a time-domain feature extraction algorithm based on feature morphology is proposed. Experiments show that this method can effectively remove unnecessary interference and amplify the characteristics of signals through normalization and coherent averaging. Since the interval of the analysis waveform is gradually narrowed. The dichroic wave is divided into characteristic shapes. It can also well extract characteristic points for the main wave, the dichroic front wave, and the pulse wave shape that is not obvious in the dichroic wave. It has the characteristics of high recognition accuracy, wide application range, and strong anti-interference ability. It can provide direct and accurate basis for clinical applications, such as non-invasive blood pressure monitoring, central pulse pressure measurement, pulse wave shape characteristic quantity K, arterial reflection wave enhancement index, etc. It is of great significance for early prevention, diagnosis, treatment and prognosis evaluation of related vascular diseases. The algorithm proposed in this paper still uses manual recognition method to recognize pulse wave morphological features, with some errors. In the future work, we will use the deep learning algorithm to classify the pulse waves according to their morphological characteristics, and then extract the time-domain features of the classified pulse waves.

5. Funding and patents

Sichuan Major Science and Technology Projects (NO. 2022ZDZX0033) provides necessary financial support for data acquisition and algorithm verification.

References

[1] Fei Cui, Xiaohui Chen and Jie Peng, A non-invasive blood viscosity detecting method based on pulse wave. MATEC Web of Conferences, 2020.
[2] Keyu Meng, Jun Chen, Xiaoshi Li,Yufen Wu, Flexible Weaving Constructed Self-Powered Pressure Sensor Enabling Continuous Diagnosis of Cardiovascular Disease and Measurement of Cuffless Blood Pressure. ADVANCED FUNCITONAL MATERIALS, 2018.
[3] K Meng, X Xiao, W Wei, Highly Sensitive Flexible Iontronic Pressure Sensor for Fingertip Pulse Monitoring. ADVANCED HEALTHCARE MATERIALS, 2022.

[4] ZhihuaChen, AnHuang, XiaoliQiang, Improved neural networks based on genetic algorithm for pulse recognition. Computational Biology and Chemistry, 2020.
[5] N Li, J Yu, H Hu, The correlation study of Cun, Guan and Chi position based on wrist pulse characteristics. IEEE Access, 2021.
[6] ZhixingJiang, ChaoxunGuo, DavidZhang, Pressure wrist pulse signal analysis by sparse decomposition using improved Gabor function. Computer Methods and Programs in Biomedicine, 2022.
[7] DongmeiLin, AihuaZhang, JasonGu, Detection of multipoint pulse waves and dynamic 3D pulse shape of the radial artery based on binocular vision theory. Computer Methods and Programs in Biomedicine, 2018.
[8] Tsai, Yun-Ning, Chang, Yu-Hsin, The use of time-domain analysis on the choice of measurement location for pulse diagnosis research. JOURNAL OF THE CHINESE MEDICAL ASSOCIATION, 2018.
[9] ZHAO Zhi-qiang, ZHENG Guo-wei, SHEN Wei, LIAO Cheng, research on pulse wave signal noise reduction and feature point identification. Electronic Design Engineering, 2013.
[10] Zhang Menglong, Li Xiaofeng Xu, Jinlin,Huang Wanfeng, Pulse wave feature extraction based on improved slop thresholding method. ELECTRONIC MEASUREMENT TECHNOLOGY, 2017.
[11] Fufeng, Feature Point Recognition Method of Pulse Signal Based on Wavelet Modulus Maxima. Computer Engineering, 2019.
[12] Wei Sun, Ning Tang, Guiping Jiang Study of Characteristic Point Identification and Preprocessing Method for Pulse Wave Signals. Journal of Biomedical Engineering, 2015.
[13] Xiangjun Huang, Wu Xing, Feng Li, Application of Syntactic Pattern Recognition in Research on Pulse Wave's Characteristic Information. Chinese Journal of Medical Instrumentation, 2015.
[14] Ji Zhong, Liu Xu, Study on feature points recognition of pulse wave based on waveform feature and wavelet. Chinese Journal of Scientific Instrument, 2016.
[15] Huang L , Geng X, Xu Hao , Zhang Y, Li Zhi ,Zhang J, and Zhang H Interference Signal Identification of Sensor Array Based on Convolutional Neural Network and FPGA Implementation. Electronics.2022.